Article

# Stoichiometric Compounds of Magnesium Dichloride with Ethanol for the Supported Ziegler–Natta Catalysis: First Recognition and Multidimensional MAS NMR Study

Piero Sozzani, Silvia Bracco, Angiolina Comotti, Roberto Simonutti, and Isabella Camurati

*J. Am. Chem. Soc.*, **2003**, 125 (42), 12881-12893• DOI: 10.1021/ja034630n • Publication Date (Web): 30 September 2003



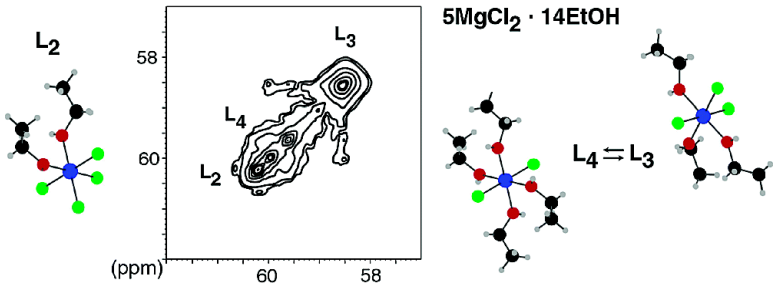


## More About This Article

Additional resources and features associated with this article are available within the HTML version:

- Supporting Information
- Links to the 4 articles that cite this article, as of the time of this article download
- Access to high resolution figures
- Links to articles and content related to this article
- Copyright permission to reproduce figures and/or text from this article

View the Full Text HTML

J|A|C|S
ARTICLES
Published on Web 09/30/2003

# Stoichiometric Compounds of Magnesium Dichloride with Ethanol for the Supported Ziegler−Natta Catalysis: First Recognition and Multidimensional MAS NMR Study

Piero Sozzani,*,† Silvia Bracco,† Angiolina Comotti,† Roberto Simonutti,† and Isabella Camurati‡

*Contribution from the Department of Materials Science, University of Milano−Bicocca, Via R. Cozzi 53, 20125 Milan, Italy, and Basell Polyolefins Italia, G. Natta Research Center, P.le G. Donegani 12, I-44100 Ferrara, Italy*

Received February 12, 2003; E-mail: Piero.Sozzani@mater.unimib.it.

***Abstract:*** Ethanol associates easily with $MgCl_2$ to form adducts of complex architecture, but until now available characterization methods have failed to identify the pure stoichiometric compounds and their structures. To remedy this, we set about applying homonuclear and heteronuclear 2D correlated solid-state NMR spectroscopy to identify the pure compounds and the ethanol-to-magnesium coordination pattern. High spinning speed and Lee-Goldburg sequences were able to reduce the hydrogen spin-diffusion and homonuclear coupling in the crystalline solid, thus achieving high resolution also in the hydrogen domain. On this basis, the pure adducts, of interest as catalyst supports for Ziegler−Natta polymerization, were isolated for the first time. Magnesium coordination sites with given numbers of ligands and their multiplicity in the crystal cells were determined in the new-found stoichiometric complexes. Variable temperature and 2D carbon−carbon exchange NMR, as well as relaxation times in the fast motion regime, revealed the disordering phenomena generated by ethanol dynamics in the crystal. Decoding the intriguing polymorphysm of the precursors permits to trace the genealogy of tailored $MgCl_2$ titanate granules, active as highly productive catalysts for the stereospecific polymerization of olefins.

## Introduction

The last generation of heterogeneous catalytic systems for the production of polyolefins is titanium tetrachloride supported on magnesium dichloride.[1] This catalytic system is the most advanced method in industrial applications, guaranteeing very high yields and the highest stereochemical control of the obtained polymers.[2] Great interest is now being focused on attempting to understand the structure of active sites. Recently, a number of relevant contributions[3] presented about the structure and the control exerted by titanium trichloride/magnesium dichloride complex on the degree of stereoregularity. In fact, the understanding of how the activated surface of magnesium dichloride can influence the properties of the sites so markedly has turned into a great challenge for today's techniques of surface science, spectroscopy, and computational methods.[4,5] The idea that magnesium dichloride simply provides a dispersing surface for the isomorphous titanium trichloride seems to be overcome. The role of the support in the heterogeneous catalysis of polyolefins is now assuming the same relevance as the role of the ligand in homogeneous catalysis.[6]

The method of preparing magnesium dichloride, supporting the Ti species, affects the catalytic properties markedly. Mechanical and chemical routes were pursued for the formation

† University of Milano − Bicocca and INSTM UdR Milano.
‡ Basell S.p.a.

(1) (a) Albizzati, E.; Giannini, U.; Collina, G.; Noristi, L.; Resconi, L. In *Polypropylene Handbook: Polymerization, Characterization, Properties, Applications*; Moore, E. P. Jr., Ed.; Hanser Publishers: New York, 1996; 11−111. (b) Moore, E. P. Jr. In *The Rebirth of Polypropylene: Supported Catalysts*; Hanser Publishers: New York, 1998; 45−71.
(2) (a) Pino, P.; Mülhaupt, R. *Angew. Chem.* **1980**, *92*, 869−887. (b) Barbè, P. C.; Cecchin, G.; Noristi, L. *Adv. Polym. Sci.* **1987**, *81*, 1−77. (c) Albizzati, E.; Giannini, U.; Balbontin, G.; Camurati, I.; Chadwick, J. C.; Dall'Occo, T.; Dubitsky, Y.; Galimberti, M.; Morini, G.; Maldotti, A. *J. Polym. Sci., Part A: Polym. Chem.* **1997**, *35*, 2645−2652. (d) Xu, J.; Feng, L.; Yang, S. *Macromolecules* **1997**, *30*, 2539−2541. (e) Chung, J. S.; Choi, J. H.; Song, I. K.; Lee, W. Y. *Macromolecules* **1995**, *28*, 1717−1718. (f) Kissin, Y. V.; Mink, R. I.; Nowlin, T. E. *J. Polym. Sci., Part A: Polym. Chem.* **1999**, *37*, 4255−4272.
(3) (a) Busico, V.; Cipullo, R., Corradini, P.; De Biasio R. *Macromol. Chem Phys.* **1995**, 196, 491−498. (b) Cavallo, L.; Guerra, G.; Corradini, P. *J. Am. Chem. Soc.* **1998**, *120*, 2428−2436. (c) Toto, M.; Morini, G.; Guerra, G.; Corradini, P.; Cavallo, L. *Macromolecules* **2000**, *33*, 1134−1140. (d) Mori, H.; Sawada, M.; Higuchi, T.; Hasebe, K.; Otsuka, N.; Terano, M. *Macromol. Rapid Commun.* **1999**, *20*, 245−250.
(4) (a) Kim, S. H.; Craig, R. T., Somorjai, G. A. *Langmuir* **2000**, *16*, 9414−9420. (b) Kim, S. H.; Somorjai, G. A. *J. Phys. Chem. B* **2001**, *105*, 3922−3927. (c) Tewell, C. R.; Malizia, F.; Ager, J. W., III.; Somorjai, G. A. *J. Phys. Chem. B* **2002**, *106*, 2946−2949. (d) Kim, S. H.; Somorjai, G. A. *J. Phys. Chem. B* **2002**, *106*, 1386−1391. (e) Magni, E.; Somorjai, G. A. *Surf. Sci.* **1996**, *345*, 1−16. (f) Mori, H.; Hasebe, K.; Terano, M. *Macromol. Chem. Phys.* **1998**, 199, 2709−2715.
(5) (a) Boero, M.; Parrinello, M.; Terakura, K. *J. Am. Chem. Soc.* **1998**, *120*, 2746−2752. (b) Boero, M.; Parrinello, M.; Hüffer, S.; Weiss, H. *J. Am. Chem. Soc.* **2000**, *122*, 501−509. (d) Martinsky, C.; Minot, C.; Ricart, J. M. *Surf. Sci.* **2001**, *490*, 237−250. (e) Seth, M.; Margl, P.; Ziegler, T. *Macromolecules* **2002**, *35*, 7815−7829. (f) Boero, M.; Parrinello, M.; Weiss, H.; Hüffer, S. *J. Phys. Chem. A* **2001**, *105*, 5096−5105. (g) Puhakka, E.; Pakkanen, T. T.; Pakkanen, T. A. *J. Phys. Chem. A* **1997**, *101*, 6063−6068.
(6) (a) Gomez, F. J.; Waymouth, R. M. *Science* **2002**, *295*, 635−636. (b) Ewen, J. A.; Jones, R. L., Razavi, A.; Ferrara, J. D. *J. Am. Chem. Soc.* **1988**, *110*, 6255−6256. (c) Ewen, J. A.; Jones, R. L.; Elder, M. J.; Rheingold, A. L.; Liable-Sands, L. M. *J. Am. Chem. Soc.* **1998**, *120*, 10 786−10 787. (d) Ewen, J. A.; Elder, M. J.; Jones, R. L.; Rheingold, A. L.; Liable-Sands, L. M.; Sommer, R. D. *J. Am. Chem. Soc.* **2001**, *123*, 4763−4773.

of "active" $MgCl_2$ loaded with the catalyst. In particular, the reaction of $MgCl_2$ with a Lewis base, typically an alcohol, treated with an excess of $TiCl_4$ can produce *super active catalyst*.[1a] The use of $MgCl_2$/EtOH adducts with a restricted range of compositions yields, after inserting the transition metal, a most efficient and selective catalytic system. The key point for the enhanced performances of the supported catalyst is the nature of the $MgCl_2$ precursors, obtained as complexes with Lewis bases, which undergo direct titanation. In fact, Lewis base/$MgCl_2$ ratios in the precursor determine, among other features, the activity and the isotacticity degree of the resulting polymer.[1b] On the contrary, a two step process involving removal of ethanol to form $MgCl_2$ and subsequent addition of $TiCl_4$ leads to modest catalytic performances. The models proposed until now refer only to the insertion of $TiCl_4$ upon the preferred cut faces of $MgCl_2$, the information about precursor structure being still lacking. Thus, the removal of ethanol from the solvate could be envisaged as a method for producing nanostructures tailored for the proper generation of the catalytic system.[1,7]

The present paper is aimed at contributing to a deeper understanding, and thereby to a greater control, of the structure of $MgCl_2$/EtOH crystalline adducts that, until now, has not been resolved, and that takes part in the catalytic system of Ziegler−Natta polymerization. To date, the $MgCl_2$ adducts formed by coordinating ethanol molecules to the metal site have been addressed by a few approaches, including X-ray diffraction, IR, and Raman.[4c,8] The comprehension of the phase behavior is far from clear, due to the intrinsic complexity of the system. The first problem is that the number of EtOH/$MgCl_2$ ratios varies greatly, being from one up to six moles of ethanol per mole of $MgCl_2$, resulting in the generation of a large number of samples of varying formal composition; no described method allows the reliable discrimination of pure compounds from mixtures. The samples are obtained as powders (especially microspheres): single crystals are only available for $MgCl_2$·6EtOH compound.[9] Furthermore, the high vapor pressure of the adducts affects the reliability of the results. Because of these impediments X-ray diffraction powder patterns do not lead unequivocally to the determination of the pure phases and their correct stoichiometry.[8,10] Despite recent efforts, vibration spectroscopy could identify only some features of the structures, such as Mg hexacoordinated to oxygen and Mg not coordinated to oxygen (pure $MgCl_2$), but the data did not discriminate between pure compounds and mixtures.[4c]

This prompted us to search for further experimental evidences by the application of advanced solid-state NMR:[11,12] the NMR data changed the previous scenario and suggested a novel structural interpretation. NMR is a method of choice when mixtures of compounds and static or dynamic disorder are present; in particular, High-Speed Magic Angle Spinning and Multidimensional NMR, that can provide high-resolution both on carbon and hydrogen domain, is sensitive to phase structure and to local interaction between nuclei. If there is enough resolution, the signal multiplicity and internal ratios can identify the structures of the pure phases.

## Experimental Section

**Preparation of the $MgCl_2$·*n*EtOH Adducts with $n < 3$.** In a glass reactor equipped with a bubble condenser, a thermometer and a stirrer with commercial $MgCl_2$ and dry EtOH was loaded in the desired stoichiometric ratio. To help the stirring, an equivalent volume of paraffin oil (OB/55) was added to the mixture. The mixture was then heated to about 120 °C, until it was clear and maintained at this temperature for 2−3 h. Excess paraffin oil was added and the molten salt was emulsified with the paraffin by increasing the stirring rate. The emulsion was quenched in a larger volume of *n*-heptane kept at −20 °C. After 1 h at this temperature, the suspension was warmed to −10 °C and held at this temperature 1 h. Finally, the temperature was slowly increased to room temperature, the solid was recovered by filtration, washed several times with *n*-hexane and dried under vacuum at room temperature. By the above procedure a powder of $MgCl_2$·3EtOH with microsphere morphology was obtained.

The $MgCl_2$·*n*EtOH samples having a ratio of $n < 3$ were prepared by dealcoholation of the sample with EtOH/$MgCl_2$ ratio equal to 3. This compound was transferred in a fluidized bed reactor and, under vacuum (5−6 mmHg) was warmed to 60 °C. A stream of dry nitrogen was passed through the compound, whereas the temperature was increased at 3 °C/h. The dealcoholation process was stopped at the desired EtOH/$MgCl_2$ ratio and the removed EtOH was collected in a cold trap and measured. The samples were prepared three times for data reproducibility. A selection of the adducts are presented here; they were subjected to dealcoholation times of 8, 12, 17, 18 and 25 h (samples h, i, j, k, l, respectively). The composition of all the complexes was checked for EtOH content by GC analysis and by elemental analysis for magnesium and clorine determination. The compositions, expressed by weight percentage, are for $MgCl_2$ and EtOH, respectively, as follows. Sample h: 43.1 and 56.9; sample i: 45.8 and 54.2; sample j: 50.7 and 49.3; sample k: 53.3 and 46.7; sample l: 59.5 and 40.5.

Hydrated samples with the controlled amount of water ($H_2O$/$MgCl_2$ molar ratios up to 0.6) were prepared starting from water/ethanol mixtures added in closed vessels to anhydrous magnesium dichloride.

**Preparation of $MgCl_2$·6EtOH and the Adducts with $n > 3$.** In a 2 L round-bottom flask equipped with stirrer, a thermometer and bubble condenser was loaded with 1.2 L of anhydrous ethanol and 95 g of anhydrous $MgCl_2$. This resulted in an exothermic reaction, and the mixture was stirred at reflux temperature for 2 h. The warm solution was filtered and then refluxed for 1 h. After cooling at 0 °C, the solution was filtered and the white crystalline solid was collected, washed with pentane and dried, giving 297 g of product ($Mg^{2+}$ = 5,1 wt %, $Cl^-$ = 19.7 wt %, EtOH = 79.9 wt %).

The dehalcoholation process of the $MgCl_2$·6EtOH adduct gives rise to samples with EtOH/$MgCl_2$ ratios ranging from 6 to 3.

**Solution NMR Analysis for the Determination of Composition.** The composition of the samples was determined by dissolving completely a weighed amount (ca. 30 mg) of the compounds h−l in 1 mL of $D_2O$ and adding a weighed amount the reference compound THF (ca. 20 mg). The $^1H$ NMR spectra, as recorded at 600 MHz on a Bruker Avance spectrometer, can resolve all the signals of ethanol and THF. The integration of the signals gives the EtOH/THF molar ratio and the absolute amount of ethanol in the given sample. Thus, EtOH/$MgCl_2$ molar ratios "*n*" are calculated. Sample h: $n = 2.73$; sample i: $n = 2.48$; sample j: $n = 2.01$; sample k: $n = 1.83$; sample l: $n = 1.45$.

**Density Measurements.** The density of the samples was determined by floating measurements. Small amounts of the samples *h* and *l* were transferred under dry nitrogen atmosphere to mixtures of hexane ($d$ = 0.659 g cm$^{-3}$) and ethylenetetrachloride ($d$ = 1.622 g cm$^{-3}$). The mixtures were prepared in order to match the density of the compounds.

(7) Forte, M. C.; Coutinho, F. M. B. *Eur. Polym. J.* **1996**, *32*, 223−231.
(8) Di Noto, V.; Marigo, A.; Viviani, M.; Marega, C.; Bresadola, S.; Zannetti, R. *Makromol. Chem.* **1992**, *193*, 123−131.
(9) Valle, G.; Baruzzi, G.; Paganetto, G.; Depaoli, G.; Zannetti, R.; Marigo, A. *Inorg. Chim. Acta* **1989**, *156*, 157−158.
(10) Bart, J. C. J.; Roovers, W. *J. Mater. Sci.* **1995**, *30*, 2809−2820.
(11) Laws, D. D.; Bitter, H. M. L.; Jerschow, A. *Angew. Chem., Int. Ed. Engl.* **2002**, *41*, 3096−3129.
(12) Brown, S. P.; Spiess, H. W. *Chem. Rev.* **2001**, *101*, 4125−4155.

Sample h shows the density of $1.22 \pm 0.01$ g cm$^{-3}$ and sample l the density of $1.43 \pm 0.01$ g cm$^{-3}$.

**X-ray Powder Diffraction.** The X-ray powder diffraction patterns were measured on a $\theta/\theta$ D8-advance powder diffractometer (Bruker) using Cu K$\alpha_1$ radiation at 40 kV, 20 mA (Bragg−Brentano geometry). The specimens were loaded on a diffractometer holder under Ar atmosphere and were protected with Nijuol. The X-ray powder diffraction patterns were recorded with a scanning speed of 0.25° $2\theta$min$^{-1}$. The pattern indexing of sample l was performed using DICVOL91.[13]

**Differential Scanning Calorimetry.** Differential scanning calorimetry (DSC) traces were performed on Mettler Toledo Star$^e$ Thermal Analysis System equipped with $N_2$ low-temperature apparatus. The experiments were run under nitrogen atmosphere in both an open Al-crucible and a hermetically sealed steel-crucible. The samples were first heated from 30 °C to 200 °C at 5 °C/min and then cooled to 30 °C at 5 °C/min, and heated up to 200 °C a second time at 5 °C/min. The sample weights for the DSC measurements were about 15 ÷ 20 mg and were measured to an accuracy of 0.05 mg.

**Solid State NMR Measurements.** The solid-state NMR spectra were run at 75.5 MHz, on a Bruker Avance 300 instrument operating at a static field of 7.04 T equipped with both 4 and 7 mm double resonance MAS probes. The samples were spun at a spinning speed of 15 kHz, and Ramped-Amplitude Cross-Polarization (RAMP-CP)[14] transfer was applied. The 90° pulse for proton was 2.9 $\mu$s (86 kHz). $^{13}$C Single Pulse Excitation (SPE) experiments were run using a recycle delay of 10 and 100 s and Cross Polarization (CP) MAS experiments were performed using a recycle delay of 10 s and a contact time of 2.5 ms. Variable temperature spectra were collected between 243 K and 367 K with 7 mm $ZrO_2$ rotors spinning at a standard speed of 5 kHz; 90° pulse for proton was 4.7 $\mu$s (53 kHz).

Phase-Modulated Lee-Goldburg (PMLG) heteronuclear $^1$H−$^{13}$C correlation (HETCOR) experiment coupled with fast magic angle spinning (MAS) allows the registration of 2D spectra with high-resolution both in the proton and carbon dimension.[15−17] Fast MAS (15 kHz spinning speed) averages the chemical shift anisotropy (CSA) of $^{13}$C nuclei and practically reduces to zero the spinning sidebands, dramatically decreasing the complexity of the carbon spectrum, especially in systems containing carbons with large CSA. Narrow proton resonances, with line widths in the order of 1−2 ppm, are obtained with homonuclear decoupling during $t_1$; this resolution permits a sufficiently accurate determination of the various proton species present in the system (for further background about LG see Supporting Information). Phase-Modulated Lee−Goldburg (PMLG)[15] $^1$H−$^{13}$C HETCOR spectra were run with LG period of 18.9 $\mu$s. The efficient transfer of magnetization to the carbon nuclei was performed applying RAMP-CP[14] sequence. Quadrature detection in $t_1$ was achieved by time proportional phase increments method. Carbon signals were acquired during $t_2$ under proton decoupling applying two pulse phase modulation scheme (TPPM).[18] The pulse sequence used in this work is reported in Figure S1a.

Two-dimensional (2D) exchange NMR is a powerful technique to investigate slow dynamic processes occurring on a time-scale up to several seconds.[19] The pulse scheme for this experiment is given in Figure S1b (for further details and the background for 2D Solid State NMR experiments see the Supporting Information). The $^{13}$C 2D-exchange NMR spectra were taken with 1024 data points along $t_2$ and with 512 points incremented of 150 $\mu$s along $t_1$. The experimental conditions for the individual NMR experiments are presented in the figure captions accompanying the respective spectra.

Crystalline polyethylene in the orthorhombic phase was taken as an external reference at 32.85 ppm from tetramethylsilane (TMS). Spectral profiles were fit by Lorentzian line shapes. The $^{13}$C spin−lattice relaxation time ($T_1$) values were obtained using the method developed by Torchia.[20] Spectra were acquired with 10 different $\tau$ values. The rotors were prepared in a drybox under nitrogen atmosphere.

## Results and Discussion

**The Identification of the Pure Compounds.** Two alternative routes for the preparation of $MgCl_2$ ethanolates are reported in the literature: (a) heating in a closed vessel of a given molar ratio of $MgCl_2$ and ethanol;[4c,10] (b) dealcoholation of crystalline $MgCl_2$·6EtOH or lower stoichiometry samples for varied times and temperatures.[8] The process leads to samples of a given formal composition, indicated in the following as *n* (where *n* is between 0 and 6 in the $MgCl_2$·*n*EtOH formula). These samples are mostly constituted by binary mixtures of pure crystalline compounds. Prior to this work a reliable methodology for identifying the pure compounds and for recognizing them in the mixtures was lacking. To this aim solid-state NMR was applied and could establish the stoichiometry of the pure compounds and the composition of the mixtures, as described in this paragraph. The crystalline adducts were characterized without alteration, as obtained in the microsphere morphology (Figure S2) by quenching the emulsion of the melted salt in paraffin.

A large number of coordinated structures formed by divalent metals and alcohols are reported.[21] For low numbers of coordinated ethanol groups, polymeric chains are formed and held together by "covalent" Metal$^{II}$-alogen-Metal$^{II}$ bonding. The polymeric chains are constituted by a distribution of octahedral sites with 1 or 2 ethanol molecules coordinated to the metal. When there are high numbers of coordinated ethanol groups, an octahedral coordination of the metal with partially or totally isolated sites is generally observed.[21,22] The octahedral sites are defined as $L_n$, according to the number of ligands on each site (where $1 < n < 6$) and are depicted in Figure 1.

The ligands are described in many instances to be arranged in a complex manner: a mix of linear and three-dimensional structures can be created and large crystal cells are produced. From the NMR spectroscopy point of view, a large number of resonances can be expected for each carbon atoms depending on the non equivalent nuclei in the unit cell.[23]

$^{13}$C Cross Polarization (CP) MAS spectra of a few $MgCl_2$·*n*EtOH adducts in the range $n = 1-3$, performed at room temperature, for the methylene and the methyl regions are presented in Figure 2.

Identical profiles are obtained by quantitative single pulse excitation (SPE) spectra with a recycle delay of 100 seconds, that guarantees the full relaxation of all the nuclei, ensuring that cross polarization MAS NMR experiments at room tem-

(13) Boulif, A.; Lonër, D. J. *J. Appl. Crystallogr.* **1991**, *24*, 287−294.
(14) Metz, G.; Wu, X.; Smith, O. S. *J. Magn. Reson. A* **1994**, 110, 219−227.
(15) Vinogradov, E.; Madhu, P. K.; Vega, S. *Chem. Phys. Lett.* **1999**, 314, 443−450.
(16) Lee, M.; Goldburg, W. I. *Phys. Rev.* **1965**, *140*, 1261−1271.
(17) van Rossum, B.-J.; Förster, H.; de Groot, H. J. M. *J. Magn. Reson.* **1997**, *124*, 516−519.
(18) Bennet, A. E.; Rienstra, C. M.; Auger, M.; Lakshmi, K. V.; Griffin, R. G. *J. Chem. Phys.* **1995**, 103, 6951−6958.
(19) Caravatti, P.; Deli, J. A.; Bodenhausen, G.; Ernst, R. R. *J. Am. Chem. Soc.* **1982**, *104*, 5506−5507.
(20) VanderHart, D. L. *J. Chem. Phys.* **1986**, *84*, 1196−1205. Torchia, D. A. *J. Magn. Reson.* **1978**, *30*, 613−616.
(21) Poonia, N. S.; Bajaj, A. V. *Chem. Rev.* **1979**, *79*, 389−445.
(22) (a)L′Haridon, P.; Le Bihan, M. T. *Acta Crystallogr.* **1973**, *B29*, 2195−2203. (b) L′Haridon, P.; Le Bihan, M. T.; Laurent, Y. *Acta Crystallogr.* **1972**, *B28*, 2743−2748. (c) Halut-Desportes, P. S.; Philoche-Levisalles, M. *Acta Crystallogr.* **1978**, *B34*, 432−435.
(23) Sozzani, P.; Comotti, A.; Simonutti, R. In *Crystal Engineering: From Molecules and Crystals to Materials*; NATO Science Series, Braga, D.; Grepioni, F.; Orpen, A. G., Eds.; Kluwer Academic Publishers: Dordrecht **1999**, *538*, 443−458.

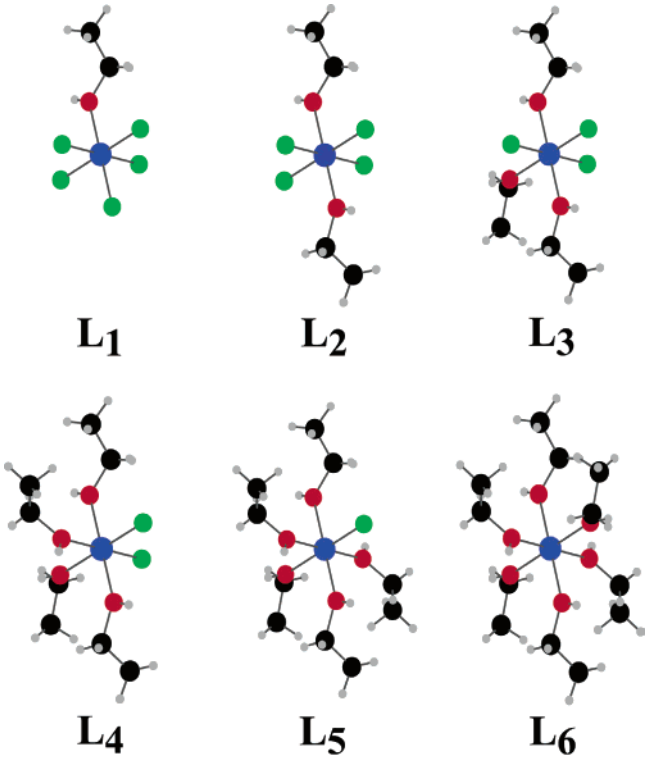


***Figure 1.*** Schematic representation of the octahedral coordination of the $Mg^{II}$ sites with a number of EtOH ligands: $n = 1 \div 6$. The sites are labeled as $L_n$ depending on the number of ligands: a single isomer is represented even if more than one structural isomer is possible.

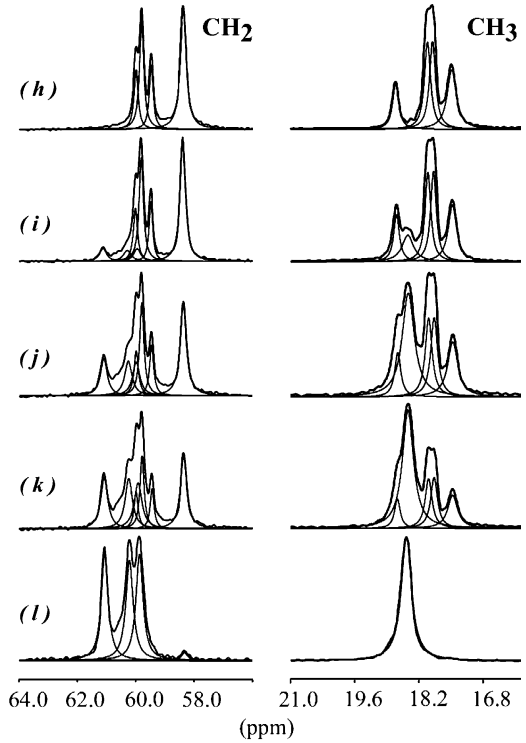


***Figure 2.*** $^{13}C$ CP MAS NMR spectra of the methylene and methyl regions of samples *h*−*l* with varying EtOH/$MgCl_2$ ratios. The spectra were recorded with a spinning speed of 15 kHz and 7.04 T magnetic field. The profiles were deconvoluted by Lorentzian line-shapes.

perature are also quantitative. A rich multiplicity of signals can be recognized as typical of each spectrum; the chemical shifts and profiles are markedly affected by the ethanol content. The

***Table 1.*** $^{13}C$ CP MAS NMR: Chemical Shifts, Assignments, and Quantitative Results

| adduct with *low* EtOH/$MgCl_2$ ratio (sample l) | | | | |
|---|---|---|---|---|
| $^{13}C$ c.s. (ppm) | assignment | % area | experimental intensities[a] | idealized intensities |
| 61.11 | $CH_2$ | 33.35 | 1.00 | 1 |
| 60.27 | $CH_2$ | 27.87 | 0.99 | 1 |
| 59.93 | $CH_2$ | 14.88 | 1.01 | 1 |
| 18.47 | $CH_3$ | | 1.00 | 1 |
| **adduct with *high* EtOH/$MgCl_2$ ratio (sample h)** | | | | |
| $^{13}C$ c.s. (ppm) | assignment | % area | experimental intensities[a] | idealized intensities |
| 59.97 | $CH_2$ | 14.75 | 1.03 | 1 |
| 59.78 | $CH_2$ | 27.87 | 1.95 | 2 |
| 59.45 | $CH_2$ | 14.88 | 1.04 | 1 |
| 58.35 | $CH_2$ | 42.50 | 2.98 | 3 |
| 18.68 | $CH_3$ | 14.57 | 1.02 | 1 |
| 17.99 | $CH_3$ | 28.28 | 1.98 | 2 |
| 17.88 | $CH_3$ | 28.49 | 1.99 | 2 |
| 17.46 | $CH_3$ | 28.66 | 2.01 | 2 |

[a] The experimental intensities (e.i.) within $CH_2$ (or $CH_3$) carbons have been calculated as follows: e.i.$= f\,(\text{Area}_i/\Sigma_i\ \text{Area}_i)$ where $f$ is the smallest integer number chosen to obtain experimental intensities close to integer numbers. $f$ is equal to 3 for the methylenes of adduct with *low* EtOH/$MgCl_2$ ratio (sample *l*) and 7 for the methylenes and methyls of adduct with *high* EtOH/$MgCl_2$ ratio (sample *h*).

chemical shift of the methylenes appears downfield compared to the reported ethanol chemical shifts in solution ($\delta = 57.79$ ppm, in a solution of 0.5 mL of EtOH and 1.5 mL of $CDCl_3$) proving the association, in the solid state, of ethanol with an electron withdrawing nucleus, like divalent magnesium. It is worth noting that the most downfield peaks appear in the samples with low ethanol content in accordance with the stronger degree of association. In addition, a downfield shift of the weighed average chemical shift of the signals is observed at decreasing ethanol content.[24]

The signals were quantified by the deconvolution analysis. In the methylene region (Figure 2) the adduct with *low* EtOH/$MgCl_2$ ratio (sample *l*) presents three signals of intensity 1.00: 0.99:1.01 (starting from downfield), indicating a simple ratio between the signals idealized as 1:1:1 (multiplicity of 3) (Table 1). On the other hand, the spectrum of the adduct with *high* EtOH/$MgCl_2$ ratio (sample *h*) is deconvoluted by four signals with an intensity ratio of 1.03:1.95:1.04:2.98 (from downfield). The internal ratio is idealized as 1:2:1:3 and the spectrum can be interpreted as the sum of seven equal parts (multiplicity of 7). Simple ratios are not recognized in samples with intermediate ratios of ethanol per mole of $MgCl_2$ (samples i, j, k), instead it can be observed that the signal at 61.11 ppm progressively decreases and the signal at 58.35 ppm progressively intensifies at increasing EtOH/$MgCl_2$ ratios. In the profile of the compound l the specific signals of the profile of the compound h are missing and viceversa.

The above observations prompted us to recognize the traces of two pure compounds in the extreme composition values of this series of samples. The deconvolution procedure could provide us with a number of Lorentzian shaped signals identified by chemical shift, intensity and line width. The two sets of signals due to the stoichiometric compounds are always present

(24) The weighed average chemical shift is the summation of the chemical shift of each deconvoluted signal multiplied by the area of each peak and divided by the area of the whole profile.

with the same internal ratio as reported above, greatly reducing the degree of freedom of the system. By this way, the intermediate profiles are fully deconvoluted with great accuracy as a given fraction of the pure profiles.

Similar results, although with somewhat less resolution, are obtained by the methyl region where a single peak is detected in the sample with *low* EtOH content, while 1:2:2:2 internal ratios are observed for the peaks of the sample with *high* EtOH content (Figure 2, samples l and h). The methyl profiles of the adducts with intermediate "*n*" ratios consist of a given proportion of profiles of the pure compounds (Table 1).

The weighed average chemical shift of each group of signals (calculated as reported in ref 24) was evaluated as a function of the ethanol content (see the Experimental Section).

A least-squares fitting procedure indicates a linear correlation (correlation coefficient of 0.96 and 0.97 for methylene and methyls, respectively). The linear dependence of the average chemical shift on the chemical composition of the samples (shown in Figure S3) is reproduced by combining the two average chemical shift values of the pure stoichiometric compounds, according to the fractions in the mixtures. The pure compounds are found at the extremes of the observed interval. The slope for methylenes is double that for the methyls, consistent with the fact that the electron withdrawing effect of Mg cation coordinated to EtOH oxygen is mostly felt by the carbon directly bonded to oxygen. Thus, the NMR average chemical shift gives, with a high degree of accuracy, an independent parameter for the determination of the composition of unknown adducts.

More information was sought through 2D heterocorrelated hydrogen−carbon experiments, spreading the signals in two dimensions and gaining high resolution also in the hydrogen domain by applying Phase-Modulated Lee−Goldburg sequence coupled with fast magic angle spinning.[25] A very high resolution is reached by these techniques that virtually suppress the dipolar coupling among hydrogens that largely dominates in rigid solids (see the Experimental Section). A few experiments were performed with contact times for cross polarization ranging from 50 $\mu$s to 10 ms. It is well established that such experiments detect correlation signals when the hydrogen-to-carbon distances are short enough.[26] The time for growing the correlation signals depends on the distance, according to the scaling law of $1/d^6$. Short contact times limit the number of correlations to the signals of neighboring atoms at less than 0.2 nm.

Spectra with short contact times show cross-peaks for hydrogen−carbon covalent bonded atoms and permit the transfer of assignments from the carbon to the hydrogen domain (Figure 3, above).

Resolution is exceptionally high for a crystalline solid (LW $\approx$ 1 ppm in the hydrogen domain). From the projections and the traces in the hydrogen domain we could determine the hydrogen chemical shift of the two pure stoichiometric compounds (see the Experimental Section) (Table 2). The $^1$H chemical shifts of the methylenes of the pure compounds are differentiated by about 0.4 ppm. Methylene hydrogen signals are sensitive to the electron withdrawing effect of magnesium with respect to the $^1$H chemical shift of EtOH in $CDCl_3$ ($CH_2$ at 3.69 ppm). A downfield shift is especially observed in sample l, when less ethanol ligands are coordinated on the metal cation, as previously discussed for carbons.

***Table 2.*** $^1$H Chemical Shifts of the Adducts Derived by High-Speed MAS-PMLG $^1$H−$^{13}$C HETCOR Experiments

| adducts | $^1$H c.s.[a] (ppm) of $CH_2$ | $^1$H c.s. (ppm) of $H_2O$ |
|---|---|---|
| sample *l* | 4.33 | |
| sample *h* | 3.89 | 5.83 |
| | | 6.32 |
| sample *k* | 4.37 (l) | |
| | 3.93 (h) | |
| sample *h*, hydrated | 4.61 | 6.37 |

[a] $^1$H chemical shifts are scaled by a factor of $1/\sqrt{3}$ according to the theory (see the Experimental Section). Methyl signals resonate at about 1.23 ppm.

Long contact times (Figure 3, below) extended the correlations to vicinal groups giving rise to new cross signals of comparable intensities: methylene hydrogens can transfer magnetization to methyl carbons (and methyl hydrogens to methylene carbons) about 2.2 Å apart on the same molecule and possibly with lower probability with intermolecular transfer to nearby molecules. A signal at about 6 ppm is detected in the hydrogen domain only in the sample with *high* $EtOH/MgCl_2$ molar ratio and is assigned to the mobile hydrogens of a minor amount of water in the sample, as discussed later.

The samples of intermediate ratios of $EtOH/MgCl_2$ allowed us to compare the hydrogen chemical shift in the same spectrum and resolve the mixtures in two dimensions. Methylene and methyl 2D HETCOR spectra of a mixture (sample k) are shown in Figure 4. The traces at 3.93 and 4.37 ppm in the hydrogen domain represent carbon spectra with the typical profiles already observed for the two pure compounds (compare to Figures 2 and 3).

Thus, resolution in the hydrogen dimension provides a method of filtering the single profiles of pure compounds, and allows us to identify the stoichiometric compounds. These results support the recognition of the pure compounds in the mixtures suggested earlier by deconvolution in the $^{13}$C spectra.

**Identification of Coordination Sites in the Asymmetric Unit of the Crystal Cell.** The interpretation of the chemical shifts of the multiple peaks and the internal intensity ratio of signals in the profiles of the pure stoichiometric compounds must be derived by the ligand arrangement in the two crystal structures. The coordinated ethanols differ mainly because of the nature of the sites (namely: $L_1$, $L_2$, $L_3$, etc., as previously defined). The conformational arrangements (defined by the dihedral angles assumed by $CH_2-O-Mg-Cl$ and $CH_3-CH_2-O-Mg$) and the spatial relationships are, for the moment, taken as minor causes of the resonance shifts. The signal assignment to the structures is based on the following: (a) the internal multiplicity of signals; (b) the chemical shift value, related to the coordination strength, that is in turn reduced by the number of ethanols at each site. The largest downfield shift is associated with a single ethanol coordinated to a magnesium cation in the species $L_1$; the ethanols in $L_2$ and $L_3$ sites resonate progressively upfield.

The crystal structure of the pure stoichiometric compound with *low* $EtOH/MgCl_2$ ratio (sample l) (Figure 5b) must contain

(25) Particular attention should be paid when the chemical shift values in $f_1$ dimension are taken into account, in fact the chemical shift dispersion is scaled by a factor of $1/\sqrt{3}$ compared to what is obtained in a $^1$H SPE spectrum; furthermore a mismatch of the Lee-Goldburg condition can lead to scaled spectra, as reported in ref 14. Therefore, the effectiveness of PMLG was confirmed by a comparison with a $^1$H SPE spectrum.

(26) van Rossum, B.-J.; de Groot, C. P.; Ladizhansky, V.; Vega, S.; de Groot, H. J. *J. Am. Chem. Soc.* **2000**, *122*, 3465−3472.

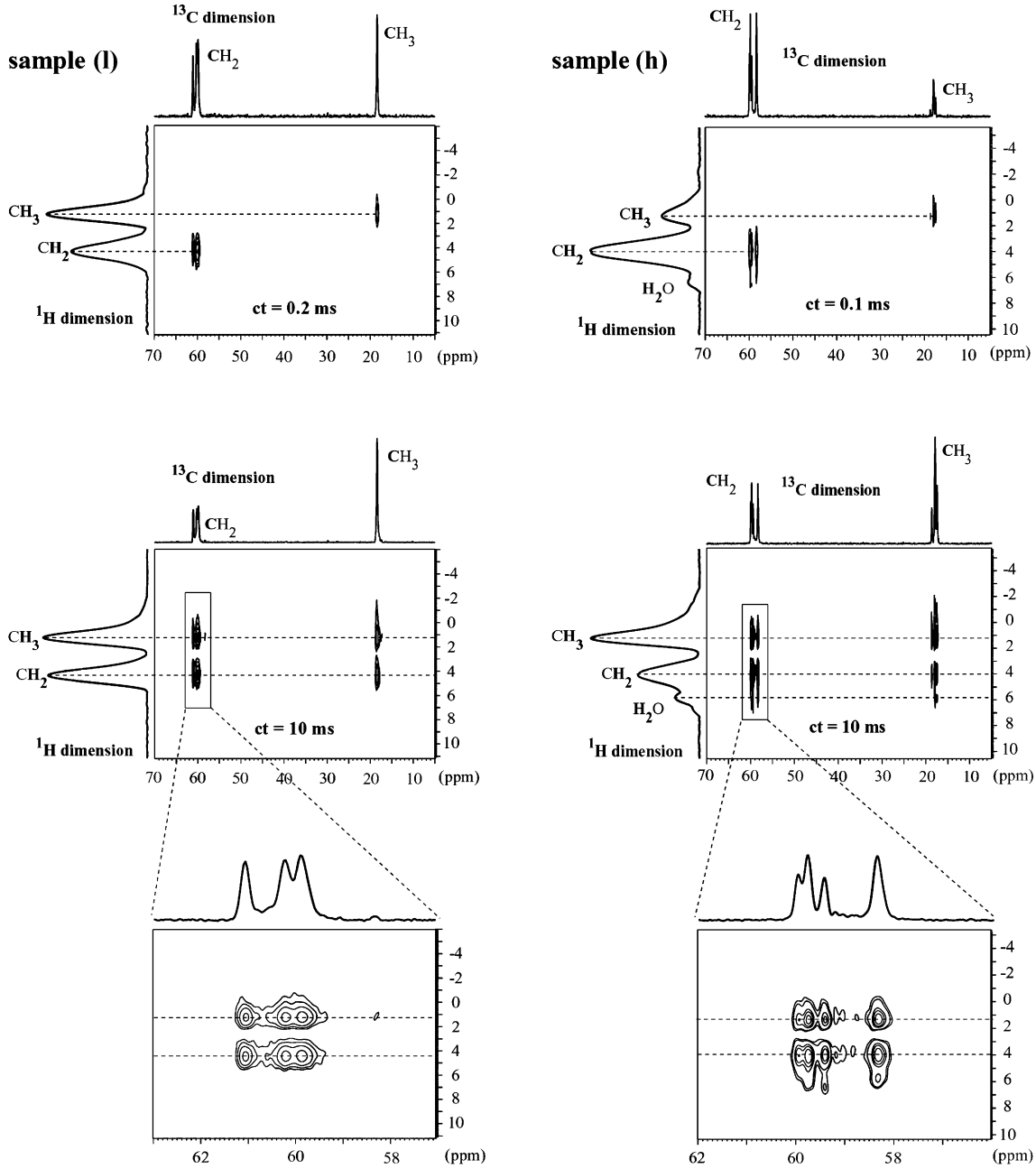


***Figure 3.*** 2D PMLG HETCOR NMR spectra, recorded with spinning speed of 15 kHz: (sample l) adduct with *low* EtOH/$MgCl_2$ ratio, and (sample h) adduct with *high* EtOH/$MgCl_2$ ratio. Respectively, short contact times of 0.1−0.2 ms (above) and long contact times of 10 ms (below) were applied for cross polarization. Projections in the $^{13}$C and in the $^{1}$H dimensions are reported along with the spectra; expansions of the 2D spectra in the carbon dimension are also represented for the methylene region.

a balance of $L_1$ and $L_2$ species to match the chemical composition within the experimental errors.

The three sharp ethanol signals of intensity 1:1:1 in the methylene spectrum detect three independent ethanol molecules; thus, the sites in the asymmetric unit of the crystal cell will be: $L_1$ and $L_2$, in the ratio of 1:1. The assignments are given in Figure 5b. The presence of two signals for the site $L_2$ is not surprising if we take into account that the two ethanols can be nonequivalent.[27] Thus, a number of 3 ethanols distributed on 2 magnesium atoms are counted, indicating the formation of the compound $2MgCl_2 \cdot 3EtOH$ ($MgCl_2 \cdot 1.5EtOH$).

The pure stoichiometric compound with *high* EtOH/$MgCl_2$ ratio (sample h) must contain species $L_2$ and those of higher order. In the methylene region, an upfield signals of intensity 3 is observed in the spectrum. The chemical shift and the intensity of 3 suggest the assignment of the upfield signal to the site $L_3$ (Figure 5a). In the downfield region, a group of signals at 59−60 ppm of total intensity 4 contains two signals with the same chemical shifts of those previously assigned to $L_2$ in the $2MgCl_2 \cdot 3EtOH$ compound. Other two signals in the middle of the spectrum are assigned to a site $L_4$ included for $^1/_2$ in the asymmetric unit cell. The chemical shift value for $L_4$ is

(27) Given the sharp and well-defined peaks, we assume that the spectrum resolves all the possible peaks and no further splitting is present, as confirmed by the variable temperature experiments shown later. As a consequence, a larger asymmetric unit that doubles that proposed is excluded. The possibility that the asymmetric unit is the half of that proposed should imply that the observed atoms lie on symmetry elements in the asymmetric unit.

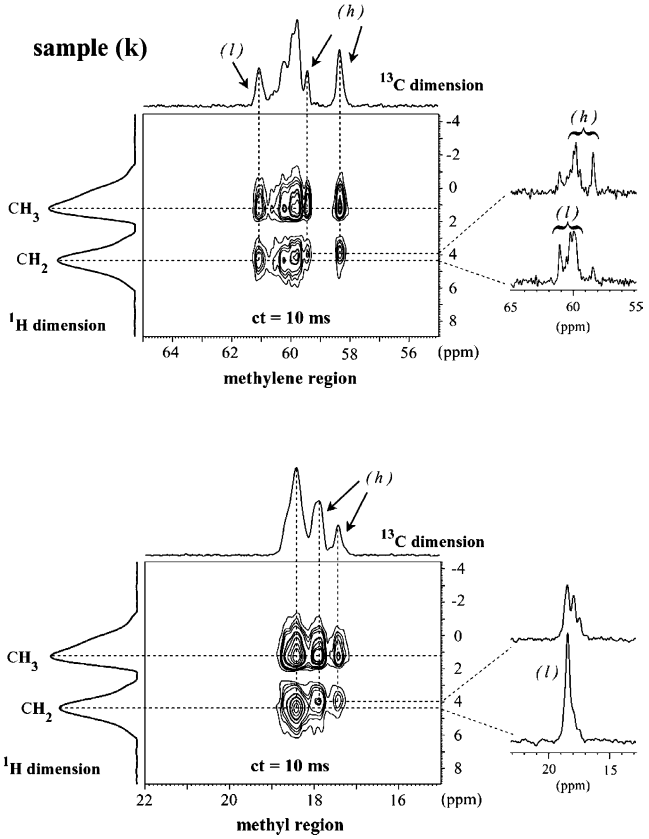


***Figure 4.*** 2D PMLG HETCOR NMR of sample k, methylene (above) and methyl (below) carbon region. Contact time of 10 ms and a spinning speed of 15 kHz are applied. Traces in the carbon domain, collected at hydrogen chemical shift of 3.93 and 4.37 ppm, are reported on the right side of the figure. Profiles similar to that of samples h or l are indicated where recognized.

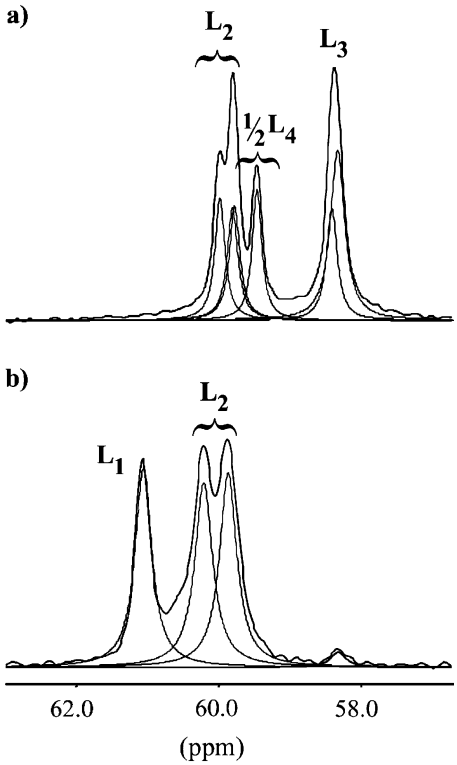


***Figure 5.*** Expanded $^{13}$C CP MAS NMR spectra and assignments of the methylene region of the identified crystalline adducts. The signals of $5MgCl_2$·14EtOH (a) and $2MgCl_2$·3EtOH (b) samples are assigned to the sites $L_n$. The deconvolution quantifies the sites included in the asymmetric unit of the crystal cells, as indicated.

consistent with the chemical shifts in samples of high stoichiometry ($3 < n < 6$), as later discussed. Thus, the asymmetric unit cell contains $L_2$, $L_3$, and $^1/_2$ $L_4$, indicating 7 ethanols distributed on 2.5 Mg sites. This establishes the stoichiometry $5MgCl_2$·14EtOH ($MgCl_2$·2.8EtOH). The stoichiometry derived by the NMR quantitative spectra is consistent with the chemical composition. The NMR results provide the exact stoichiometry following on directly from the determination of the content of the asymmetric unit, as conventionally obtained by the X-ray single-crystal resolution of the crystal structure.

**Variable Temperature MAS NMR Experiments and Mobility of the Ethanol Ligands.** The experiments performed from low to high temperature are reported in Figures 6−7 for the two pure compounds $2MgCl_2$·3EtOH and $5MgCl_2$·14EtOH. At high temperature, the highest symmetry and dynamically averaged arrangements are obtained: in fact, raising the temperature leads to the merging of peaks. The ethanols become more similar at high temperature because exchange phenomena are more likely to occur. Variable temperature experiments reveal that the structures are affected by dynamic disorder, which may explain the interpretation difficulties encountered with X-ray diffraction.

In particular, the compound $2MgCl_2$·3EtOH shows, for methylenes, variable patterns composed by three signals of the same intensity. The signals of the ethanols $L_2$ overlap perfectly only at low temperature. At high temperature, one $L_2$ signal tends to merge with $L_1$ toward a single chemical shift (Figure 6). This is a first observation that the ethanol molecules are not fixed in a single conformation but are sensitive to the temperature and any given species $L_n$ dynamically explore several conformations departing from the stable ones at low temperature. The close contiguity of sites along the polymeric Mg−Cl chains imposes a motion coherence between vicinal ethanols, to minimize the steric interactions. Large librations or fast conformational exchange fairly explain the signal merging with temperature. Similar effects have been observed in diethoxy- or diethyl-substituted polymers before thermotropic phase transitions.[28] The short relaxation times ($^{13}$C $T_1$ of 12 s in the extreme narrowing limit) at room temperature are consistent with the occurrence of motion components faster than the MHz regime.

The $5MgCl_2$·14EtOH compound behaves intriguingly. At low temperature (243 K), both methylene and methyl regions present a rich multiplicity of signals (Figure 7).

The intensities of the signals follow integer numbers as low as one or occasionally two, indicating that almost any single ethanol in the asymmetric unit is resolved. The multiplicity, as determined by deconvolution, is consistent for methylenes and methyls and confirm that at any temperature the asymmetric unit contains seven ethanols and at least six of them differ in chemical shifts. The total number of seven confirms the presence of ethanols arranged on sites $L_2$, $L_3$, and $L_4$ in the asymmetric unit, as discussed above (see, for reference, Figure 5a).

In the methylene region, below 283 K (Figure 7), the above sites and conformations are well resolved. In $5MgCl_2$·14EtOH

(28) (a) Crosby, R. C.; Haw, J. F. *Macromolecules* **1987**, *20*, 2324−2326. (b) Meille, S. V.; Farina, A.; Gallazzi, M. C.; Sozzani, P.; Simonutti, R.; Comotti, A. *Macromolecules* **1995**, *28*, 1893−1902.

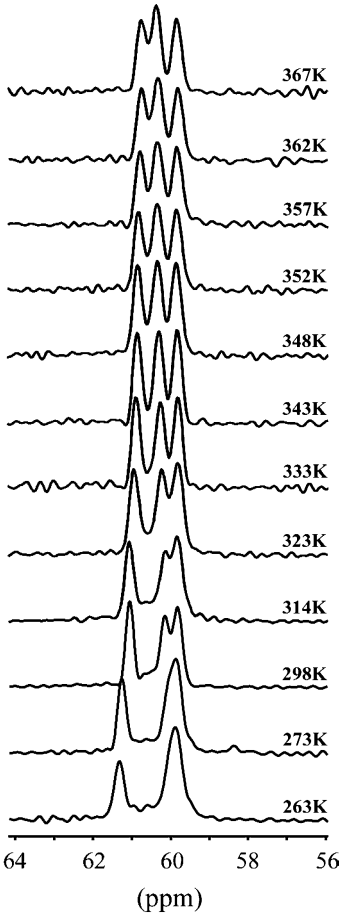


***Figure 6.*** Variable temperature $^{13}C$ CP MAS NMR spectra of methylene region of $2MgCl_2 \cdot 3EtOH$ compound from 367 K to 263 K.

adduct, raising the temperature, all the peaks merge into groups of accumulated intensity (Figure 7) and the signals due to high coordination sites tend to disappear. Above 315 K, the signal $L_3$ progressively vanishes from the methylene spectrum. At 353 K the CP MAS NMR spectra of the methylenes and methyls become very weak; instead intense signals are detected in the SPE MAS NMR signals shown in the Figure 7. This is an indication that $^1H-^{13}C$ dipolar coupling, needed for the cross polarization, is weak due to the presence of almost isotropic ethanol mobility. On cooling back to room temperature the spectra are reproduced without hysteresis, describing a reversible process.

To understand the reason for this behavior we applied a 2D exchange NMR experiment, that is a method of choice for the study of slow exchange phenomena in the range from milliseconds to seconds. 2D-exchange NMR in rotating solids was successfully applied in several cases to demonstrate exchange phenomena in polymers and in organic materials.[29] The experiments have been performed at a few mixing times from 0.3 to 5 s. The expanded methylene regions of the 2D-NMR spectra are reported together with the total projection profile in the carbon domain (Figure 8).

The spectra show exchange signals at 2 s between the $L_3$ and the $L_4$ peaks, at longer mixing times the exchange signals between the $L_3$ and $L_4$ peaks are intensified. At a mixing time of 0.3 s, no exchange signals are revealed. The behavior clearly

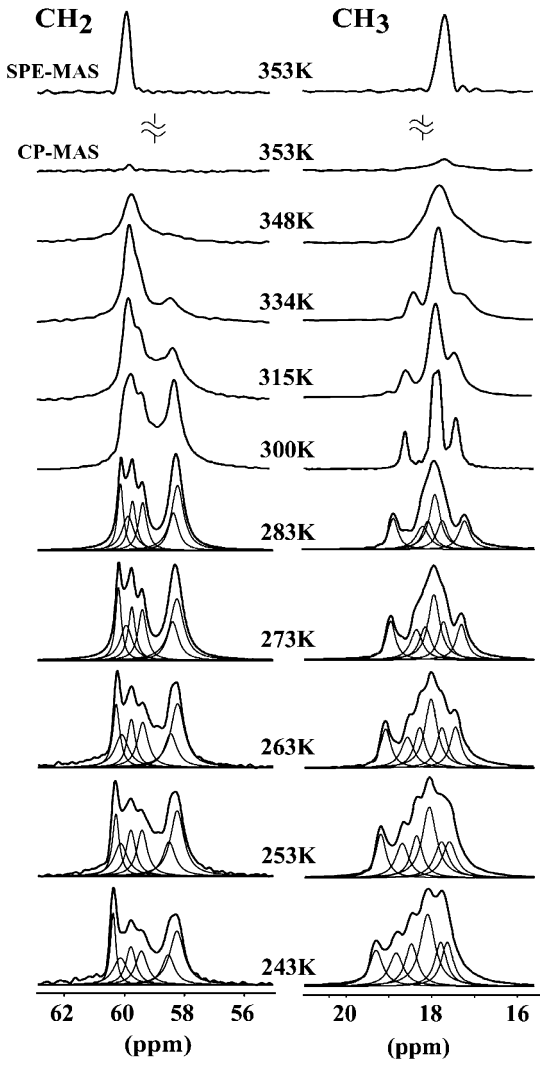


***Figure 7.*** Variable temperature $^{13}C$ CP MAS NMR spectra of the methylene and methyl regions of $5MgCl_2 \cdot 14EtOH$ adduct: from 353 K to 243 K. The spectra were deconvoluted by Lorentzian line-shapes.

demonstrates that $L_4$ species are transformed into $L_3$ species by a slow equilibrium $L_4-L_3$, involving the reversible removal of an ethanol molecule coordinated to magnesium.

As a conclusion of the 2D-exchange experiments, the exchange behavior involves not only the commutation among conformations on a site but also between sites, resulting in a complex exchange dynamics. The spin−lattice relaxation time measurements performed at room temperature show $^{13}C$ $T_1$ as low as 2 and 12 s (for methyls and methylenes, respectively), suggesting an efficient relaxation in the hundreds of MHz regime. The fast motion regime detected by relaxation measurements is most likely due to the conformation interchange on a single site.

**X-ray Powder Diffraction.** X-ray powder diffraction patterns of selected samples are presented in Figure S4. The reflections of the pure adducts present at $2\theta$ values lower than 15° $d$ spacing of 14.367, 9.943, 9.003, and 8.648 Å for the $5MgCl_2 \cdot 14EtOH$ compound, and 11.480, 8.632, and 7.234 Å for the $2MgCl_2 \cdot 3EtOH$ compound.

The samples previously identified as mixtures present a larger number of X-ray reflections that, from the knowledge of the pure compound profiles, can be labeled as belonging to one or

(29) Schmidt-Rohr, K.; Spiess, H. W. *Macromolecules* **1991**, *24*, 5288.

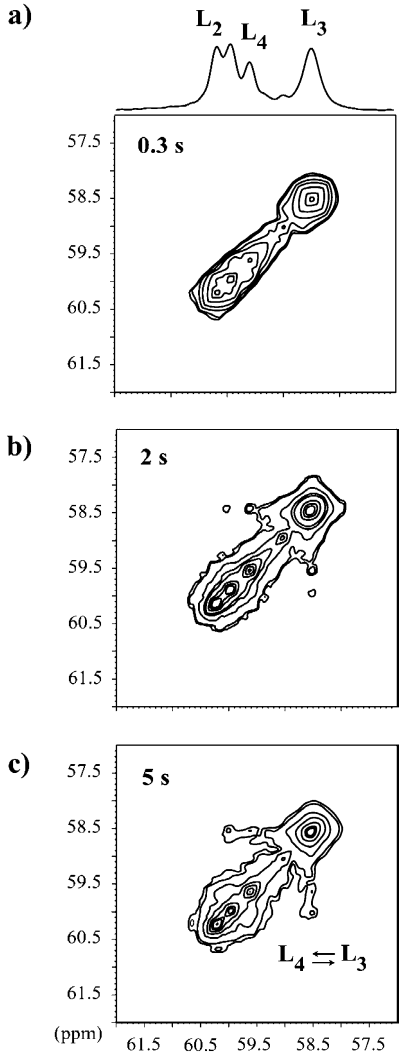


***Figure 8.*** CP MAS $^{13}C$ 2D exchange spectra of the methylene region of $5MgCl_2 \cdot 14EtOH$ at room temperature with the following mixing times: (a) 0.3 s; (b) 2 s; and (c) 5 s.

the other pure pattern; in fact, no signal overlapping is present at $2\theta$ values lower than 15°. The intensities of the X-ray reflections follow qualitatively the fraction of the pure adducts in the mixtures. However, without an independent identification the recognition of pure compounds from mixtures by X-ray powder diffraction patterns would have been tentative.[10]

In the range of stoichiometry ratios ($n = 1 \div 3$), $M^{II}$ metal chlorides (where the metal cation can be Co, Mn, Ni, or Mg) coordinated with alcohols form chains of octahedral sites lying one next to the other.[21,22] We can assume similar behavior by the ethanol ligands of $Mg^{II}$. The type and number of $L_n$ sites present in the asymmetric unit and whether they lie in a general or in a special position have been above established by NMR for both the pure compounds. From the powder diffraction pattern of $5MgCl_2 \cdot 14EtOH$ sample a large unit cell is suggested by the presence of low $2\theta$ reflections. The powder diffraction pattern recorded for our $5MgCl_2 \cdot 14EtOH$ sample presents a strong analogy to that of a structure of the same stoichiometry based on manganese. In the $5MnCl_2 \cdot 14EtOH$ case, the single-crystal refinement was performed and a triclinic unit cell with $P\bar{1}$ space group was proposed ($a = 10.68$ Å, $b = 10.58$ Å, $c = 16.73$ Å, $\alpha = 62.30°$, $\beta = 107.0°$, $\gamma = 109.20°$).[22] The asymmetric unit cell contains an enchainment of $L_2$, $L_3$, and $L_4$ sites (the $L_4$ site lying on the inversion center and thus weighted for $^1/_2$). Similarly, in $5MgCl_2 \cdot 14EtOH$ sample, 2.5 sites were counted by NMR in the asymmetric unit as $L_2$, $L_3$, and $^1/_2$ $L_4$ (again with the $L_4$ site lying on a special position). Therefore, a triclinic unit cell with the space group $P\bar{1}$ was considered for the cell parameter refinement from the X-ray powder peaks after they had been indexed according to ref 22a. The refined unit cell parameters are $a = 10.755(3)$ Å, $b = 10.497(3)$ Å, $c = 16.542(3)$ Å, $\alpha = 62.20(2)°$, $\beta = 107.60(2)°$, $\gamma = 109.88(2)°$, $V = 1530.1(4)$ Å$^3$ and the calculated density ($d = 1.22$ g cm$^{-3}$) is in excellent agreement with the experimental density of the crystalline powder obtained by floating measurements ($1.22 \pm 0.01$ g cm$^{-3}$).

The X-ray diffraction profile of the $2MgCl_2 \cdot 3EtOH$ compound (Figure S4) could be indexed considering a monoclinic unit cell that gives the following least-squares refinement cell parameters: $a = 22.99(2)$ Å, $b = 9.32(1)$ Å, $c = 7.15(1)$ Å, $\beta = 92.7°(1)$ ($V = 1530.88$ Å$^3$). The content of the asymmetric unit is determined independently from NMR data as sites $L_1 + L_2$ and, under the hypothesis of four formula units per unit cell ($Z = 4$), the density of 1.43 g cm$^{-3}$ is calculated, in agreement with the experimental measurement of $1.43 \pm 0.01$ g cm$^{-3}$. From the single-crystal structure refinement a triclinic unit cell was proposed for the manganese chloride derivative $2MnCl_2 \cdot 3EtOH$ (space group = $P\bar{1}$, $Z = 2$, $a = 10.80$ Å, $b = 9.57$ Å, $c = 7.95$ Å, $\alpha = 107.33°$, $\beta = 81.37°$, $\gamma = 102.04°$, $V = 762.6$ Å$^3$).[22b] It contains two formula units instead of four in half the volume of $2MgCl_2 \cdot 3EtOH$ and the asymmetric unit shows $L_1 + L_2$ sites as in the magnesium-based compound. The proposed structure of the $2MnCl_2 \cdot 3EtOH$ was described as an extended enchainment of $L_1$ and $L_2$. Thus, infinite polymer chains of octahedral magnesium sites are suggested also for $2MgCl_2 \cdot 3EtOH$ compound.

**Hydrated Compounds.** It is known that even small amounts of water are absorbed by the strongly hygroscopic magnesium chloride derivatives. Water can remove chlorine atoms from the coordination sphere of magnesium. Adding various amounts of water in the preparation of the mixtures (see the Experimental Section), the $^{13}C$ MAS NMR ethanol spectra give rise to additional signals identified both in the methylene and methyl spectra (Figure S5).

A progressive diminishing of the $5MgCl_2 \cdot 14EtOH$ profile is observed with increasing amount of water, and disappears with a water/$MgCl_2$ molar ratio of 0.6 (Figure S5a and S5e). A novel group of signals at 59.10, 58.79 ppm for methylenes and at 18.56, 18.17, 17.92, and 17.67 ppm for methyls increases progressively. The signals with the same internal intensity ratio were recognized in all the mixtures containing various amounts of water together with the profiles of the pure compound $5MgCl_2 \cdot 14EtOH$ (Figure S4b–d). Due to the cation–water affinity the additional water removes chlorine atoms from some magnesium sites, producing the novel hydrate crystal structure.

The powder X-ray diffraction patterns of the hydrated samples show the presence of both the characteristic reflections of $5MgCl_2 \cdot 14EtOH$ and of the hydrated structure (Figure S6a). At low $2\theta$ value (<15°), the reflections with $d$ spacing of 9.612, 9.298, 7.407, 6.805, 5.262, and 4.526 Å do not overlap those of the $5MgCl_2 \cdot 14EtOH$ and are diagnostic of the hydrated phase. At high water content (0.6 $H_2O/MgCl_2$ molar ratio) the X-ray

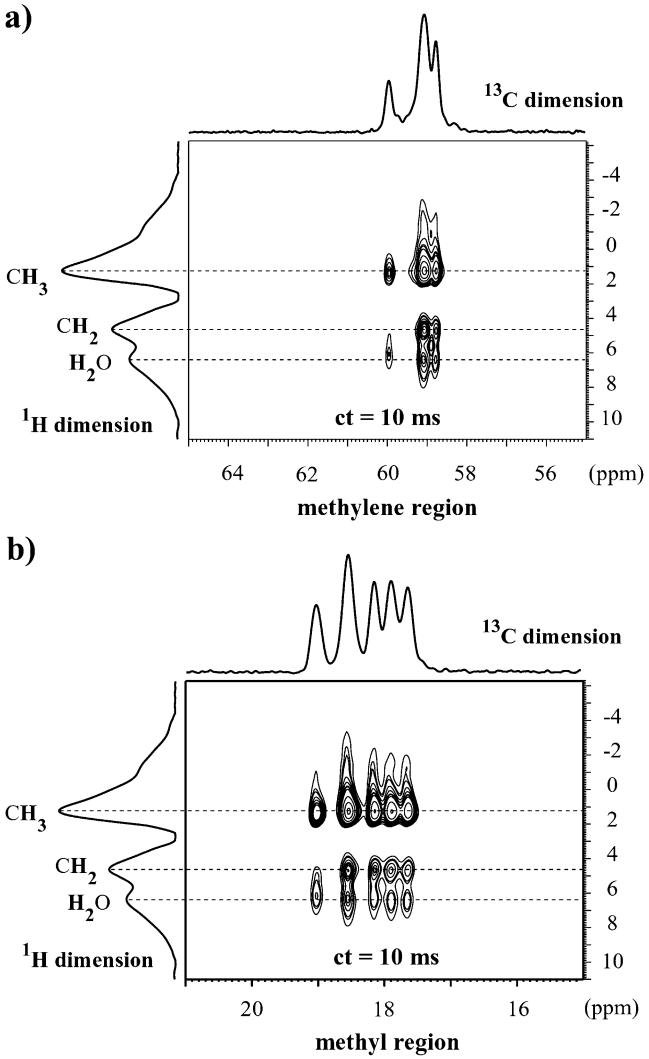


***Figure 9.*** 2D PMLG HETCOR of $5MgCl_2 \cdot 14EtOH$ with 0.6 $H_2O/MgCl_2$ molar ratio: (a) methylene region; (b) methyl region. Contact times of 10 ms and a spinning speed of 15 kHz are applied.

profile shows no peaks belonging to the $5MgCl_2 \cdot 14EtOH$ phase (Figure S6b), in agreement with NMR data.

To confirm the presence of $H_2O$ on the sites, 2D PMLG HETCOR NMR experiments on the sample with 0.6 $H_2O/MgCl_2$ molar ratio were performed: the hydrogen dimension shows intense peaks due to the hydrogens belonging to $H_2O$ (Figure 9). The $H_2O$ hydrogens are correlated to both methyls and methylenes and are therefore at less than one nanometer from the carbon atoms. The carbon methylene signals at 59.10, 58.79 ppm and the carbon methyls at 18.56, 18.17, 17.92, and 17.67 ppm show identical hydrogen profiles, identifying a single hydrated crystalline phase. The water can be removed from the samples with low water content by heating to 363 K in the NMR rotor and cooling to room temperature. At the end of the process, the spectrum is consistent with the pure $5MgCl_2 \cdot 14EtOH$ compound.

**Adduct $MgCl_2 \cdot 6EtOH$.** During the search for additional pure stoichiometric compounds, samples of ethanol/magnesium dichloride with formal compositions from 3 to 6 were explored. The ligands in the compounds of higher stoichiometry are weakly associated to the Mg cation and the manipulation requires great care in keeping the samples almost constantly

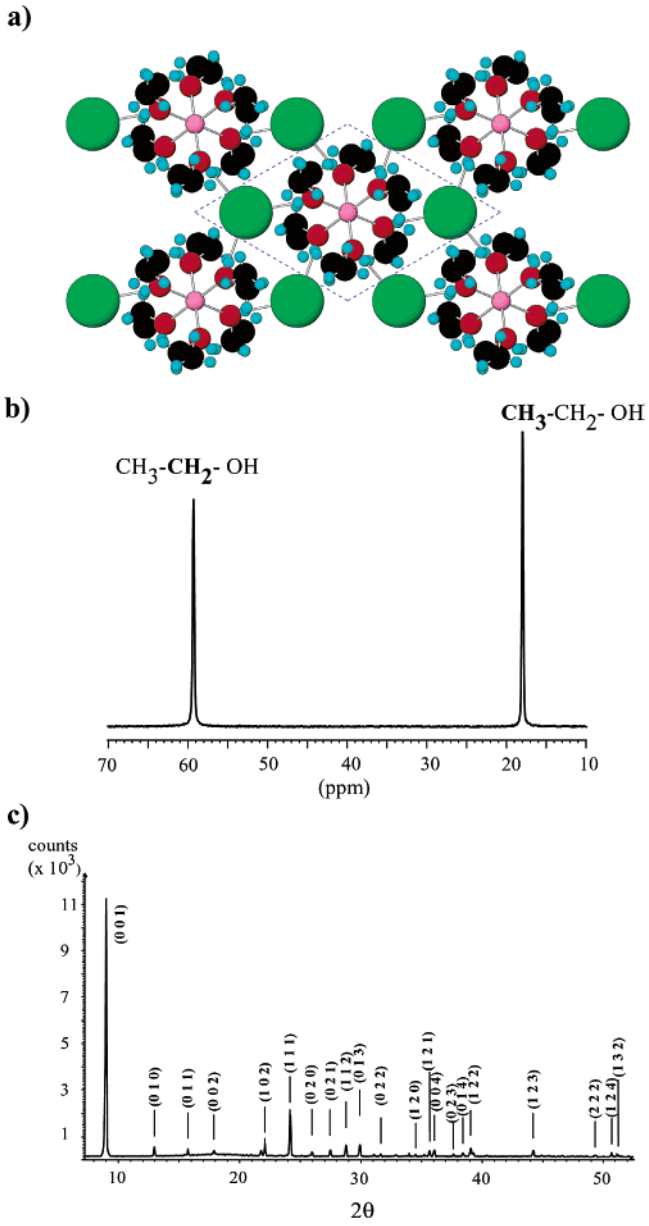


***Figure 10.*** $MgCl_2 \cdot 6EtOH$ adduct: (a) the crystal structure from the single-crystal X-ray diffraction;[9] (b) $^{13}$C CP MAS NMR spectrum; (c) X-ray powder diffraction profile with Miller indices.

under the controlled vapor pressure of ethanol. The profile of $5MgCl_2 \cdot 14EtOH$ is recognized in samples with $EtOH/MgCl_2$ ratios up to 4. At higher ratios the spectra are featureless and single peaks for each carbon atom at about 59 and 18 ppm appear. The $^{13}$C NMR spectra are simplified because the thermal motion of the coordinated ethanols is already fast at room temperature, and conformation and site averaging lead to single peaks.

Extremely sharp peaks are detected at the extreme upper limit of stoichiometry with $EtOH/MgCl_2$ ratio of 6 (Figure 10b). The sample of $MgCl_2 \cdot 6EtOH$ is a pure stoichiometric compound: the crystal structure is already known as obtained by a single-crystal analysis.[9] The experimental powder X-ray diffraction pattern, shown in Figure 10c, is indexed considering the trigonal unit cell with the space group $P\bar{1}$ and the cell parameters, refined by least-squares analysis, are $a = 7.930(2)$ Å; $c = 9.948(3)$ Å; $V = 541.755$ Å$^3$. The structure is highly symmetric and

magnesium is completely surrounded by equivalent ethanols (Figure 10a). No proximity is described for any chlorine ions to magnesium. The single peaks shown for methyls and methylenes in our NMR spectrum give support to the high-symmetry arrangement. The 2D PMLG NMR experiment is shown in the Supporting Information (Figure S7), where single hydrogen peaks are detected for the methylene and methyl. Even at low temperature the carbon and hydrogen signals do not split.

The single chemical shift values can be obtained either by the dynamic disorder of the ethanols or by equivalent arrangements adopted in the unit cell (according to the symmetry operations admitted by the space group $P\bar{1}$). Large thermal anisotropic displacements of the ethanols, detected in the single-crystal analysis,[9] do not exclude the presence of disorder. The NMR spin−lattice relaxation times are a valuable support to solve mobility problems in the crystals and were measured at various temperatures. For methylenes, they are as long as 39 s at room temperature, decrease constantly to a shallow minimum in the order of seconds at about 230 K and further increase lowering the temperature. This is an indication for a fast motional process at room temperature (over $10^{-10}$ $s^{-1}$ correlation times) that slows down to $10^{-8}$ $s^{-1}$ at 230 K. The striking results are in favor of a liquidlike motion of the ethanol molecules occurring in the crystal, even at much lower temperatures than the ethanol freezing point. The ethanol molecules surrounding magnesium atoms are very mobile but retain anyway a certain degree of anisotropy during the motion, accounting for the efficient hydrogen−carbon polarization transfer (the relaxation times are the same as measured by cross-polarization experiments and inversion−recovery SPE experiments). The shallow minimum in the relaxation curve versus temperature indicates that a wide dispersion of motion frequencies is explored by the ethanols and only a fraction of them can match the Larmor frequency of 75 MHz. In fact, the identical ethanols do not experience isolated motions, that should match the Larmor frequency at a precise temperature and should produce a deep relaxation-time minimum. More likely, a combination of motion frequency are set, where groups of atoms are geared together, and the correlation times depend on the dimensions of the coherence domains.

**Stability with Temperature and Dissociation of Ethanol from the Identified Compounds.** Calorimetric (DSC) and thermogravimetric (TGA) analyses were performed starting from 0 to 200 °C in sealed and open crucibles. Figure S8 shows the scans of the pure compounds in sealed crucibles. The pure compounds show a simple behavior, whereas the DSC traces of some mixtures are complex, as reported in Figure S9. $5MgCl_2{\cdot}14EtOH$ sample shows a single endothermic peak at 100 °C, absorbing 106 J/g (Figure S8b). A second scan shows an exotherm transition at about 80 °C followed again by the endothermic peak at 100 °C (see insert of Figure S8b). This is an indication of the reversible dissociation of this adduct with temperature under pressure of ethanol vapors, as was above demonstrated by variable temperature NMR. The decomposition happens in a single step without the formation of intermediate compounds because the rearrangement of one structure into another of lower stoichiometry is impeded for kinetic reasons. To form lower stoichiometry structures the dealcoholation must be conducted slowly under the conditions indicated in the experimental part. Kinetically controlled rearrangements or reassociation of ethanol from the gas phase are in fact observed during the thermal treatments (see inserts of Figure S8): the exothermic peaks of the formation of the adducts occur during the second heating run, because a metastable dissociated system ($MgCl_2$ + EtOH) is formed by fast cooling from 200 °C. Complex behavior was shown in open crucibles exposed to mild nitrogen flux: ethanol evolution was detected by both calorimetric and thermogravimetric analysis from 70 to 220 °C. The weight loss is dependent on the heating rate; thus, the evolution process in open crucibles is dominated by diffusion processes.

The $2MgCl_2{\cdot}3EtOH$ compound shows two DSC endothermic transitions, as performed in closed crucibles, at about 120 and 150 °C (Figure S8a). The transition temperature, higher than that recorded in $5MgCl_2{\cdot}14EtOH$ sample, is consistent with the stronger coordination bond of ethanols in the crystal structures containing a distribution of sites $L_n$ with low $n$. The enthalpy associated with the transitions is, respectively, 20 and 50 J/g. Again, the DSC and TGA runs in open crucibles led to a multiplicity of signals. A treatment of the sample in closed crucibles to a temperature of 200 °C eliminates, on the second run, the high-temperature peak (Figure S8a, insert). Instead, an exotherm of crystallization, followed by the endothermic dissociation of the latter crystal structure at 100 °C, is observed as for the $5MgCl_2{\cdot}14EtOH$ sample. After cooling and residence for a long time at room temperature, the signal at 150 °C reverts again to the original intensity (not shown). During this slow process, the two separate phases of $5MgCl_2{\cdot}14EtOH$ and $MgCl_2$ are equilibrated to one homogeneous phase of $2MgCl_2{\cdot}3EtOH$, thermodynamically stable at the given stoichiometry. On the other hand, the first transition of $2MgCl_2{\cdot}3EtOH$ is easily reversible, indicating a solid−solid transition (Figure S10).

Much lower dissociation temperature (85 °C) is shown by the adduct with the higher stoichiometry ratio $MgCl_2{\cdot}6EtOH$ (Figure S8c). The dissociation temperature is almost as low as the boiling point of liquid ethanol, consistent with the very weak association of ethanols to the matrix, confirming the large degree of motion experienced by the ethanols at room and higher temperatures.

## Conclusions

It has long been known that magnesium dichloride and ethanol, among the most widespread compounds in nature, can easily form crystalline adducts. Prior to this work the composition and structure of these crystalline compounds had not been determined. The lack of single crystals and the uneasy decoding of the XRD powder profiles prevented the recognition of adducts of specific stoichiometry from mixtures. We believe this has been a serious drawback for the basic knowledge and the development of applications.

A further reason for novelty of the present study relies on the method: suitable advanced solid state NMR techniques (1D and 2D NMR) were applied to the delicate terrain of recognizing the crystal asymmetric unit in polycrystalline samples by the evaluation of the distribution of signal multiplicities. The use of NMR as a special tool for crystallography, to be exploited in uneasy cases (especially when large and low symmetry unit cells are examined), is becoming more and more attractive.[30] High-resolution MAS NMR provides a number of constraints that can be integrated into the structure hypothesis. In the present paper, the assignment of the signals to the coordination sites

and the direct counting of the independent atoms, supported the unambiguous recognition and the description of the structures of the $MgCl_2 \cdot n$EtOH crystalline adducts. Some XRD patterns previously assigned to compounds were in fact demonstrated by the present methodology to be mixtures. Also, solid-state NMR experiments were invaluable for tracing a rich picture of the conformation and exchange dynamics of the coordinated ligands in the polycrystalline samples.

Our study could take advantage of the novel approach for better understanding the forth generation Ziegler−Natta catalytic systems, which exploit the properties of magnesium chloride modified by Lewis bases, and are currently of global industrial use.[2] In particular, we have identified for the first time the structures of the active precursors formed by magnesium chloride and ethanol, aiming at the rationale design of super-active supported Ziegler−Natta catalysts.

The process for the preparation of active and stereospecific supported catalysts has undergone a constant evolution. Novel chemical routes have overcome the pristine mechanical processes based on simple milling of $TiCl_4$ and $MgCl_2$ and extremely high activity of the catalysts has been obtained modifying the support with Lewis base ligands coordinated to the metal site. However, the best performance is reached when the transition metal is inserted without first removing the ligand or removing it partially, achieving simultaneously the titanation and formation of the active $MgCl_2$, by a process called *direct titanation*.[1b] The yield of the catalyst and the tacticity of the polymer depend markedly upon the Lewis base/$MgCl_2$ ratio when titanation occurs, suggesting that the control over the $MgCl_2 \cdot n$EtOH structure of the precursor is the key point for tailoring the catalyst activity. Thus, the elucidation of precursor structures and the identification of pure adducts singled out from the mixtures, currently described as numerous poorly defined pseudo-polymorphs, was specifically addressed by the present study. The adducts were characterized in the intact morphology of microspheres as they form by cooling paraffin emulsions. The spherical morphology of the support has been a substantial industrial achievement, because it provided the control over the morphology of the derived polymer which duplicates the form of the catalyst by an intriguing replica effect.[1b]

After this work, we are able to assert that the $MgCl_2$/EtOH ratios of 2.8 and 1.5 represent stoichiometric values of defined and stable $MgCl_2 \cdot n$EtOH complexes. The discovery of the compound formed at 2.8 ratio explains the independent observations that ethanol/magnesium chloride formulations with ratios of about 3 are the starting compositions desirable for preparing highly productive catalysts by direct titanation.[31] The index of isotacticity is very high when propene is polymerized, suggesting that the intricate architecture of highly alcoholated and exchangeable magnesium sites, here proposed, is specific for building up active surfaces for catalyst insertion. Controlled dealcoholation of the precursor to lower content of ethanol has been observed to reduce yields and tacticity of homopolymers; but the catalyst becomes suitable for ethylene-propylene copolymer production. At formulations with ethanol content lower than 1.5, the microspheres provide a porous reaction bed (*reactor-granule technology*) where more than one monomer can be polymerized to form easy-processable polyolefin alloys.[32] This might be explained by the structure of the support, here determined: at EtOH/$MgCl_2$ ratios of 1.5 the complex is in fact arranged into infinite chains of octahedral magnesium atoms connected by chlorine atoms. The continuous ribbons of $L_1$ and $L_2$, that can be indicated as *polymer chains*, are surrounded by a soft bed of mobile ethanols. The mobile nanophase is easily accessible to the titanium chloride diffusing in it: the polymer chains are not much restructured to a compact form of $MgCl_2$, when the ethanol is removed. Thus, the process is able to build up a spongy and porous structure with a remarkable surface area.

By the above observations, it can be deduced that the precursor structure has a strong influence on the surface structure and morphology of the catalyst, generating proper surfaces for titanium insertion. We suggest that the formation of $MgCl_2$/$TiCl_4$, as produced with $MgCl_2$/Lewis base complexes, keeps the memory of the ligand distribution in the precursor, in that the coordination sites occupied by titanium in $MgCl_2$ reflects the distribution of the sites of the $MgCl_2$/EtOH precursor. Up to now, scarce attention has been paid to this point, because of the lack of determination of the $MgCl_2 \cdot n$EtOH structures. As a consequence, the conventional description of the catalyst generation suffers this gap of knowledge and takes into consideration essentially the insertion of titanium chloride on the plain cut-surfaces of crystalline $\alpha$-$MgCl_2$, i.e., the (110) and (100) faces.[5,33] To implement the oversimplified view, the arrangements of the precursor coordination-sites could be taken into account for generating refined models.[34] Indeed, the role of defective structures has already been highlighted because the early times of the supported catalysis: it has been stated that the key ingredient of the catalyst is the 'activated' or $\delta$-$MgCl_2$, which exhibits a disordered structure arising from the translation and rotation of the structural Cl−Mg−Cl layers with respect to one another, that destroy the crystal order in the stacking direction.[35] In other words, the role of extended and point defects is stressed as a critical factor for the efficiency of the $MgCl_2$ supports. Our tenet is that an appropriate distribution of *defects* can be generated specifically by the precursor architecture when penetrated by the catalytic species. It is not surprising, because

(30) (a) Fyfe, C. A.; Brouwer, D. H.; Lewis, A. R.; Villaescusa, L. A.; Morris, R. E. *J. Am. Chem. Soc.* **2002**, *124*, 7770−7778. (b) Loiseau, T.; Mellot-Draznieks, C.; Sassoye, C.; Girard, S.; Guillou, N.; Huguenard, C.; Taulelle, F.; Ferey, G. *J. Am. Chem. Soc.* **2001**, *123*, 9642−9651. (c) P. Sozzani, A. Comotti, R. Simonutti, S. Bracco, A. Simonelli In *Strength from Weakness: Structural Consequences of Weak Interactions in Molecules, Supermolecules, and Crystals*; NATO Science Series, Domenicano, A.; Hargittai, I., Eds.; Kluwer Academic Publishers: Dordrecht **2002**, *68*, 319−333. (d) Comotti, A.; Simonutti, R.; Bracco, S.; Castellani, L.; Sozzani, P. *Macromolecules* **2001**, *34*, 4879−4885. (e) Sozzani, P.; Comotti, A.; Simonutti, R.; Meersmann, T.; Logan, J. W.; Pines, A. *Angew. Chem., Int. Ed. Engl.* **2000**, *39*, 2695−2698. (f) Sozzani, P.; Simonutti, R.; Galimberti, M. *Macromolecules* **1993**, *26*, 5782−5789. (g) Comotti, A.; Simonutti, R.; Catel, G.; Sozzani, P.; Chem. Mater. **1999**, *11*, 1476−1483. (h) Comotti, A.; Simonutti, R.; Sozzani, P. *Chem. Mater.* **1996**, *8*, 234−2348. (i) Comotti, A.; Gallazzi, M. C.; Simonutti, R.; Sozzani, P. *Chem. Mater*. **1998**, *10*, 3589−3596.

(31) Sacchetti, M.; Govoni, G.; Clarrocci, A. US Patent 5,221,651, June 22, 1993.

(32) (a) Govoni, G.; Clarrocci, A.; Sacchetti, M. US Patent 5,231,119, July 27, 1993. (b) Cecchin, G.; Guglielmi, F.; Pelliconi, A.; Burgin, E. US Patent 5,286,564, February 15, 1994.

(33) (a) Monaco, G.; Toto, M.; Guerra, G.; Corradini, P.; Cavallo, L. *Macromolecules* **2000**, *33*, 8953−8962. (b) Busico, V.; Corradini, P.; Ferraro, A.; Proto, A.; Savino, V.; Albizzati, E. *Makromol. Chem.* **1985**, *186*, 1125−1131. (c) Chien, J. C. W.; Weber, S.; Hu, Y. *J. Polym. Sci., Part A: Polym. Chem.* **1989**, *27*, 1499−1506.

(34) Work in progress by some of the authors.

(35) Giannini, U. *Makromol. Chem. Suppl.* **1981**, *5*, 216.

even the otherwise inert (001) face of α-$MgCl_2$ has been recently activated by the defects induced upon electron irradiation.[4e,36]

Although the target of producing tailored catalysts has been hit by a proper choice of dealcoholation technologies, there still remains much to understand for fine-tuning the desired structure of active $MgCl_2$ by the control of the alcohol complexes.

**Acknowledgments.** We are indebted to Dr. F. Piemontesi and to Dr. D. Evangelisti for the preparation of the samples and to Dr. G. Morini for helpful discussions. The help of Dr. F. Castiglione was greatly appreciated. We are grate to the late Dr. U. Giannini for precious suggestions derived by his deep knowledge of the subject. We appreciated the technical assistance of BRUKER Biospin and of S. Steuernagel. PRIN2000, Agenzia2000-CNR and BASELL are acknowledged for the financial support.

(36) Costuas, K.; Parrinello, M. *J. Phys. Chem. B* **2002**, *106*, 4477−4481.

**Supporting Information Available:** The additional information is constituted by a background and pulse sequences for Solid State 2D NMR Experiments (Figure S1); micrograph reporting the microsphere powder morphology (Figure S2); linear correlation of weighed average chemical shift of $^{13}C$ CP MAS NMR spectra vs composition of samples h−l. (Figure S3); XRD profiles of the pure adducts and mixtures (Figure S4); $^{13}C$ CP MAS NMR spectra of hydrated samples (Figure S5); XRD profiles of hydrated samples (Figure S6); 2D PMLG NMR spectrum of $MgCl_2$·6EtOH sample (Figure S7); DSC scans of the pure adducts (Figure S8); DSC scans of samples i, j, and k (S9); DSC scans and thermal cycles of $2MgCl_2$·3EtOH sample (S10). This material is available free of charge via the Internet at http://pubs.acs.org.

JA034630N